

**RIGOROUS DESIGN AND EFFICIENT OPTIMIZATION  
OF QUARTER-WAVE TRANSFORMERS IN METALLIC  
CIRCULAR WAVEGUIDES USING THE  
MODE-MATCHING METHOD AND THE GENETIC  
ALGORITHM**

**R. Thabet and M. L. Riabi**

Laboratory of Electromagnetism and Telecommunications  
University of Constantine  
25000, Algeria

**M. Belmeguenai**

Institute of Fundamental Electronics  
CNRS UMR 8622, University of Paris XI  
91405 Orsay France

**Abstract**—This paper presents an approach for the design and optimization of pseudo-gradual transitions in circular waveguides using the genetic algorithm (GA). The characterization of these transitions is carried out by the mode-matching method. This method, associated with the generalized scattering matrix technique, leads to determine the reflection coefficient on the useful band of the studied structures and to observe their frequential behavior. The GA is employed to optimize the choice of geometrical parameters by minimizing a cost function, corresponding to the maximum magnitude of the reflection coefficient in the band. The selection of the most relevant parameters allowed an improvement of the performances for the optimized components. Results of optimization are given for both two and four-section transformers.

## **1. INTRODUCTION**

In this paper, we propose a general algorithm for the characterization and the optimization of pseudo-gradual transitions in metallic circular waveguides, using the mode-matching method coupled to a genetic algorithm (GA).

Several studies, using various numerical techniques of analysis, were developed for solving the waveguide discontinuities problem: the multimode network representation [1], the finite element method [2], the scattering matrix representation [3], the multimodal variational analysis [4], the method of moments (Galerkin technique) [5] for irises analysis, and others [6]. Among the employed techniques, the mode-matching method [7–10] is appropriate for mode step discontinuities.

This method requires that the electric and magnetic fields in each side of the discontinuity be expressed by their modal expansion. This representation is followed by application of the continuity conditions at the interfaces of the junction region to match fields. This procedure, in conjunction with the orthogonality property of normal modes leads to the generalized scattering S-matrix, therefore, to determine the reflection and transmission coefficients of incident fundamental mode and higher-order modes for both TE and TM modes excited at the discontinuity. Higher order mode interactions are rigorously taken into account.

The mode-matching method has been applied with success for the design of a number of passive microwave components with multiple-step discontinuities such as the filters, transformers, irises, directional couplers, etc. The characterization of these structures is carried out by computing the generalized scattering matrix of each discontinuity, then, cascading the different matrix taking into account the length between them.

In [8], the author has presented a modal analysis of a simple and multiple discontinuities in circular waveguides. In this work, the electromagnetic field at the discontinuity is described only by  $TE_{1x}$  and  $TM_{1x}$  modes with  $x = 1, 2 \dots$

In the first part of this paper, and on the basis of [8], we describe the analysis method applied for S-parameters computation of multiples steps discontinuities in circular waveguides. The resulting algorithm is fast and accurate and has been used for modeling inhomogeneous quarter-wave transformers [11] and a good agreement is obtained with reference structures [10].

In the second part of this paper, the objective will be to optimize the parameters defining the geometrical dimensions of the studied transformers in order to obtain the best performances while minimizing the cost. Thus, the study is reformulated as a problem of optimization.

The GA [12, 13] is then applied to search for the optimal parameters in order to minimize the maximum reflection coefficient in the useful band while respecting certain constraints on dimensions. The mode-matching method calculates the magnitude of maximum reflection coefficient in the band and the GA minimizes it.

The GA is classed in the category of the global optimization techniques. These techniques are robust towards problems with several local optima and in the presence of the constraints of discontinuities and derivability. They usually converge to the global optimum of the problem. They can constitute an Interesting alternative to the traditional techniques of optimization when these do not manage to provide reliable results.

During the last years, GA techniques have been used for solving a variety of problems in electromagnetic applications such as antennas [14], filters, multilayered structure such as frequency-selective surfaces [15]. In 2000, Chiu and Chen applied the GA to reconstruct the shape and conductivity of a metallic object through knowledge of a scattered field [16]. Lai and Jeng have developed a good way to design compact and high-performance dual-band bandpass filters with microstrip lines. They optimize a scheme, based on hybrid-coded GA techniques, which is capable of searching appropriate circuit topology and the corresponding electrical parameters with dual-band characteristic [17]. Nishino and Itoh, in 2002, introduce an evolutionary generation of microwave line-segment circuits [18]. They use the GA for optimizing topology and dimensions of these circuits. The procedure also guarantees that the size of the optimized circuit is smaller than the size specified in advance.

In all these works and other ones, the GA has showed a great flexibility and efficiency.

## 2. THEORY

### 2.1. Formulation of the Problem

Consider the transformer in circular waveguide shown in Fig. 1(a). It is composed of  $N$  sections and  $N + 1$  uniaxial discontinuities. Our objective is to find [19]:

$$\hat{U} = \min_{\Phi}(U) = \min_{\Phi} \left\{ \max_{f_{\min} < f < f_{\max}} [|\Gamma(\Phi, f)|] \right\} \quad (1)$$

Where

$$\Phi = (R_1, l_1, R_2, l_2, \dots, R_N, l_N) \quad (2)$$

$R_k$  and  $l_k$  are the radius and length of the  $k$ th section for  $k = (1, 2, \dots, N)$ ,  $\Gamma$  is the reflection coefficient at the transformer input.  $f_{\min}$  and  $f_{\max}$  represent the lower and upper edges of the useful band, respectively. The purpose is to find the optimal set of parameter values of  $\Phi$  corresponding to the minimum of  $U$ , which is the maximum magnitude of  $\Gamma$  in the useful band (Figure 1(b)).

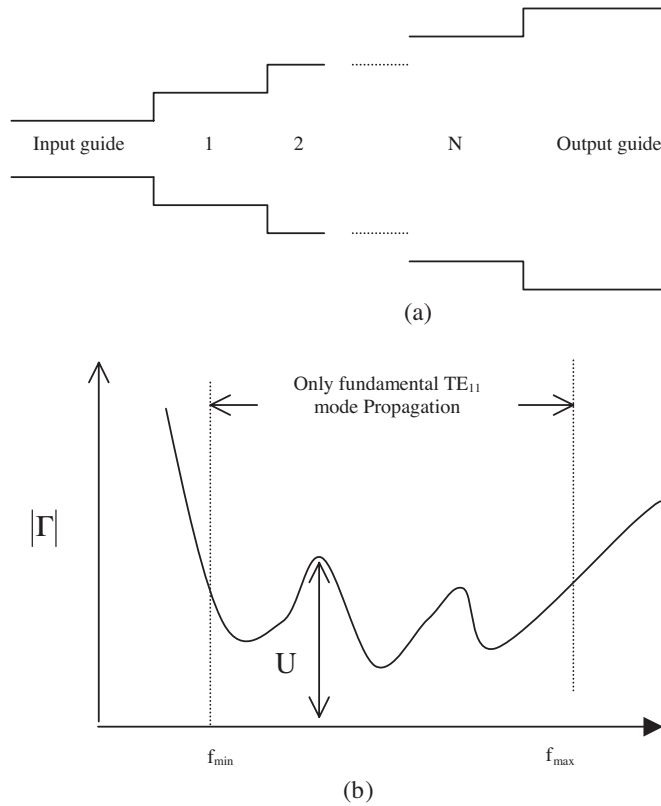


**Figure 1.** (a)  $N$ -section transformer. (b) The function  $U$  to be minimized in the useful band.

## 2.2. Technical Analysis

We present the basic formulation of the mode-matching method to calculate the generalized scattering matrix  $S$  for a transversal junction between two circular waveguides as illustrated in Fig. 2. The  $z$ -axis is the axis of symmetry for both guides and  $z = 0$  represents the plane of discontinuity. The  $TE_{11}$  mode is the incident mode in waveguide 1. The discontinuity causes the excitation of higher order modes. In the case of junction between two axially circular waveguides, only the  $TE_{1r}$  and  $TM_{1r}$  modes with  $r = 1, 2, \dots$  are excited [8]. For all following calculations, we consider only these modes. We will first recall the expressions obtained in the case of a single junction, and then derive from the equations the expressions of the complete structure reflection and transmission operators for multiples steps discontinuities.

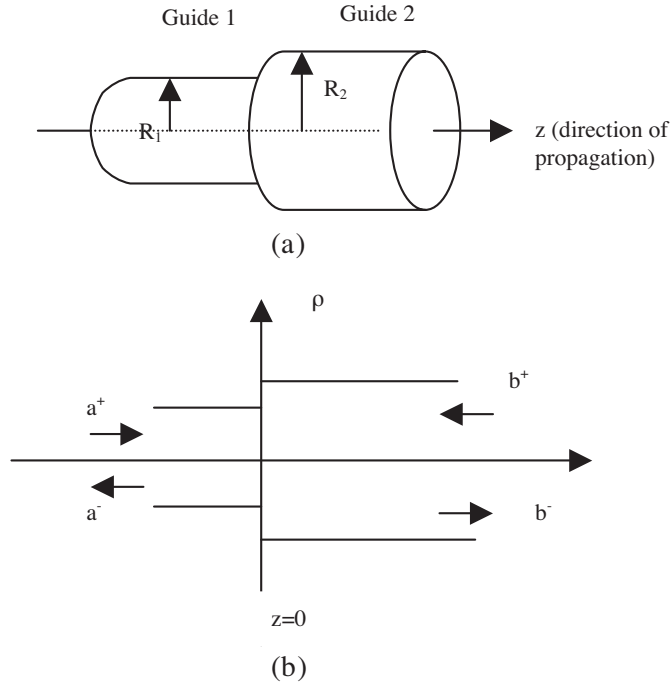


**Figure 2.** (a) Single junction in circular waveguides. (b) Reflected and transmitted waves at the junction ( $z = 0$ ).

2.2.1. Single Waveguide Junction

The procedure for obtaining the scattering matrix  $S$  of the junction is the same that one used in [20]. The electric and magnetic fields are decomposed according to the transverse electric (TE) and transverse magnetic (TM) eigenmodes. The tangential electric field just to the left of the junction ( $z = 0$ ) is given by:

$$\vec{e}_1(\rho, \theta) = \sum_n \left[ a_n^{(h)} \vec{e}_{1,n}^{(h)}(\rho, \theta) + a_n^{(e)} \vec{e}_{1,n}^{(e)}(\rho, \theta) \right] \quad (3)$$

For the region just to the right of  $z = 0$ , it is given by:

$$\vec{e}_2(\rho, \theta) = \sum_m \left[ b_m^{(h)} \vec{e}_{2,m}^{(h)}(\rho, \theta) + b_m^{(e)} \vec{e}_{2,m}^{(e)}(\rho, \theta) \right] \quad (4)$$

$a_n^{(h)(or(e))}$  and  $b_m^{(h)(or(e))}$  are the field amplitudes in the first and the second guide respectively.

The modal field at the junction ( $z = 0$ ) for a given mode  $r$  of type  $h(\text{TE})$  or  $e(\text{TM})$  in guide 1 or 2 is:

$$\vec{e}_{i,r}^{(h)}(\rho, \theta) = N_{i,r}^{(h)} \left[ \frac{1}{\rho} J_1(\beta'_{i,1r} \rho) \cos \theta \cdot \vec{i}_\rho - \beta'_{i,1r} J_1'(\beta'_{i,1r} \rho) \sin \theta \cdot \vec{i}_\theta \right] \quad (5)$$

$$\vec{e}_{i,r}^{(e)}(\rho, \theta) = N_{i,r}^{(e)} \left[ \beta''_{i,1r} J_1'(\beta''_{i,1r} \rho) \cos \theta \cdot \vec{i}_\rho - \frac{1}{\rho} J_1(\beta''_{i,1r} \rho) \sin \theta \cdot \vec{i}_\theta \right] \quad (6)$$

where  $i = 1, 2$ : corresponding to waveguides 1 and 2 respectively.

$J_1$  and  $J_1'$  are the Bessel functions and its derive of first species and first order.

$$N_{i,r}^{(h)} = \frac{\sqrt{\frac{2}{\pi}}}{\sqrt{(\beta'_{i,1r} R_i)^2 - 1} \cdot J_1(\beta'_{i,1r} R_i)} \quad \text{and} \quad N_{i,r}^{(e)} = \frac{\sqrt{\frac{2}{\pi}}}{\beta''_{i,1r} R_i \cdot J_2(\beta''_{i,1r} R_i)} \quad (7)$$

$N_{i,r}^{(h)}$  and  $N_{i,r}^{(e)}$  are normalization constants in which  $x'_r = \beta'_{i,1r} R_i$  and  $x_r = \beta''_{i,1r} R_i$  are, respectively, the  $r$ th roots of  $J_1'(x)$  and  $J_1(x)$ .

The electromagnetic boundary conditions imposed on the transverse electric fields at the plane of junction ( $z = 0$ ) are such that:

$$\vec{e}_2(\rho, \theta) = \begin{cases} \vec{e}_1(\rho, \theta) & 0 < \rho \leq R_1 \\ 0 & \text{elsewhere} \end{cases} \quad (8)$$

The scalar multiplication of (8) by  $\vec{e}_{2,m}^{(h)}(\rho, \theta)$  and integration over the circular cross section of guide 2 leads, after the use of the orthogonality properties of the normal modes, to the following expressions:

$$b_m^{(h)} = \sum_n \left[ H_{mn} a_n^{(h)} + HE_{mn} a_n^{(e)} \right] \quad (9)$$

Where:

$$H_{mn} = \int_0^{2\pi} \int_0^{R_1} \vec{e}_{2,m}^{(h)}(\rho, \theta) \cdot \vec{e}_{1,n}^{(h)}(\rho, \theta) \rho d\rho d\theta$$

and

$$\begin{aligned} HE_{mn} &= \int_0^{2\pi} \int_0^{R_1} \vec{e}_{2,m}^{(h)}(\rho, \theta) \cdot \vec{e}_{1,n}^{(e)}(\rho, \theta) \rho d\rho d\theta \\ &= 0 \end{aligned} \quad (10)$$

In the same way, multiplying (8) by  $\vec{e}_{2,m}^{(e)}(\rho, \theta)$  and integrating over the cross section of guide 2, we obtain:

$$b_m^{(e)} = \sum_n \left[ EH_{mn} a_n^{(h)} + E_{mn} a_n^{(e)} \right] \quad (11)$$

Where:

$$EH_{mn} = \int_0^{2\pi} \int_0^{R_1} \vec{e}_{2,m}^{(e)}(\rho, \theta) \cdot \vec{e}_{1,n}^{(h)}(\rho, \theta) \rho d\rho d\theta$$

and

$$E_{mn} = \int_0^{2\pi} \int_0^{R_1} \vec{e}_{2,m}^{(e)}(\rho, \theta) \cdot \vec{e}_{1,n}^{(e)}(\rho, \theta) \rho d\rho d\theta \quad (12)$$

Equations (9) and (11) lead to the matrix  $[M]$  given by:

$$b = [M]a \Leftrightarrow \begin{bmatrix} b^{(h)} \\ b^{(e)} \end{bmatrix} = \begin{bmatrix} [H] & [0] \\ [EH] & [E] \end{bmatrix} \begin{bmatrix} a^{(h)} \\ a^{(e)} \end{bmatrix} \quad (13)$$

where  $a^{(h)(or(e))}$  and  $b^{(h)(or(e))}$  being the modal weighting coefficients vectors in guide 1 and 2 respectively, the elements of the submatrices  $[H]$ ,  $[HE] = [0]$ ,  $[EH]$  and  $[E]$  are respectively the TE-TE, TE-TM, TM-TE and TM-TM E-field mode-coupling coefficients at the junction.

For the magnetic field, an analog expression to (13) can be obtained.

For numerical computation, the matrix equations are truncated to  $N$  and  $M_1$  expansion terms in guide 1 and 2, respectively. These values correspond to the number of modes necessary to achieve convergence of the S-parameters.

The  $E$ -field modal coefficient scattering matrix  $[S]$  of the junction is defined as:

$$\begin{bmatrix} a^- \\ b^- \end{bmatrix} = \begin{bmatrix} [S_{11}] & [S_{12}] \\ [S_{21}] & [S_{22}] \end{bmatrix} \begin{bmatrix} a^+ \\ b^+ \end{bmatrix} \quad (14)$$

Where  $(-)$  and  $(+)$  are used respectively for the scattered and incident waves. The expressions of the submatrices of  $S$  are given by:

$$\begin{aligned} [S_{11}] &= ([YL] + [Y_1])^{-1}([Y_1] - [YL]) \text{ and } YL = [M]^T[Y_2][Y_2][M][Y_1]^{-1} \\ [S_{12}] &= 2([YL] + [Y_1])^{-1}[M]^T[Y_2] \\ [S_{21}] &= [Y_2][M][Y_1]^{-1}([I] + [S_{11}]) \\ [S_{22}] &= [Y_2][M][Y_1]^{-1}[S_{12}] - [I] \end{aligned} \quad (15)$$

$[I]$  is the identity matrix and  $[Y_i]$  is the modal admittance matrix (for the  $i$ th guide) defined as:

$$[Y_i] = \begin{bmatrix} [Y_i^{(h)}] & [0] \\ [0] & [Y_i^{(e)}] \end{bmatrix} \quad \text{for } i = 1 \text{ or } 2, \quad (16)$$

where  $[Y_i^{(h)}]$  and  $[Y_i^{(e)}]$  are diagonal submatrices which the elements are the root square of the  $\text{TE}_{1r}$  and  $\text{TM}_{1r}$  mode admittances respectively.

$$Y_{i,1r}^{(h)} = \sqrt{\frac{\sqrt{(\beta_{i,1r}'^2 - k_0^2)}}{jk_0 N_0}} \quad \text{and} \quad Y_{i,1r}^{(e)} = \sqrt{\frac{jk_0}{N_0 \sqrt{(\beta_{i,1r}'^2 - k_0^2)}}} \quad (17)$$

With  $k_0 = \frac{2\pi}{\lambda_0}$ ,  $N_0 = 120\pi$  and  $\lambda_0$  represents the free space wavelength.

The generalized scattering matrix  $S$  determined bellow characterizes the jump in the cross section between two circular waveguides.

### 2.2.2. Multiple Waveguide Junctions

For a structure using many transitions in cascade, we use the principle of the association of the  $S$  matrices [21, 22].

Let  $\mathbf{S}^{(1)} = \begin{bmatrix} [\mathbf{S}_{11}^{(1)}] & [\mathbf{S}_{12}^{(1)}] \\ [\mathbf{S}_{21}^{(1)}] & [\mathbf{S}_{22}^{(1)}] \end{bmatrix}$  be the scattering matrix of the first

junction and  $\mathbf{S}^{(2)} = \begin{bmatrix} [\mathbf{S}_{11}^{(2)}] & [\mathbf{S}_{12}^{(2)}] \\ [\mathbf{S}_{21}^{(2)}] & [\mathbf{S}_{22}^{(2)}] \end{bmatrix}$  be the one of the second. These

two junctions are related by a waveguide  $k$  of length  $L$ .

The transmission-line matrix  $[S_L]$  of the waveguide  $k$  is a diagonal matrix such that:

$$[S_L] = \begin{bmatrix} [S_L^{(h)}] & [0] \\ [0] & [S_L^{(e)}] \end{bmatrix} \quad (18)$$

with sub matrices diagonal elements given by [20]:

$$\begin{aligned} S_{1r,1r}^{(h)} &= \exp\left(-\sqrt{\beta_{k,1r}'^2 - k_k^2} \cdot L\right) \\ S_{1r,1r}^{(e)} &= \exp\left(-\sqrt{\beta_{k,1r}''^2 - k_k^2} \cdot L\right) \end{aligned} \quad (19)$$



The expressions of the overall scattering matrix  $S^d$  are as follow:

$$\begin{aligned}
 [S_{11}^d] &= [S_{11}^{(1)}] + [S_{12}^{(1)}][S_L][U_2][S_{11}^{(2)}][S_L][S_{21}^{(1)}] \\
 [S_{12}^d] &= [S_{12}^{(1)}][S_L][U_2][S_{12}^{(2)}] \\
 [S_{21}^d] &= [S_{21}^{(2)}][S_L][U_1][S_{21}^{(1)}] \\
 [S_{22}^d] &= [S_{22}^{(2)}] + [S_{21}^{(2)}][S_L][U_1][S_{22}^{(1)}][S_L][S_{12}^{(2)}]
 \end{aligned} \tag{20}$$

where:

$$[U_1] = ([I] - [S_{22}^{(1)}][S_L][S_{11}^{(2)}][S_L])^{-1}$$

and

$$[U_2] = ([I] - [S_{11}^{(2)}][S_L][S_{22}^{(1)}][S_L])^{-1}$$

### 2.3. Genetic Algorithm

The genetic algorithms are stochastic global-search algorithms. They use the iterative optimization procedure in order to optimize a given behavior, defined by the user and expressed in the form of function, called fitness function.

This procedure begins by creating an initial random population of  $M$  individuals or chromosomes. Each chromosome represents the coding of a data set  $X$ , where:

$$X = (x_1, x_2, \dots, x_L)$$

This data set corresponds to a potential solution to the problem to be solved. The generation of a new population from the preceding one is carried out in three stages.

- a) Evaluation: the fitness function is estimated for all the chromosomes in the current population, based on certain characteristics that are desired in the solution. In our problem, it corresponds to evaluate the frequency response of a transformer. The fitness value is defined by the function  $U$  described in the equation (1). It is given by:

$$U = \max_{f_{\min} < f < f_{\max}} [|\Gamma(f)|] \quad \text{where} \quad \Gamma(f) = S_{11}(f)$$

This function  $U$  corresponds to the maximum magnitude of the reflection coefficient for the fundamental  $TE_{11}$  mode in the useful band and it is calculated by the mode-matching method.

The best data set, corresponding to the best chromosome in the population of the  $g$ th generation, belongs to the smallest  $U$ . The fitness function represents the only link between the physical problem and the GA.

- b) Selection: after the evaluation of every chromosome in the population, the selection is applied. Two parents are generated by one of the selection methods. In our case, the determinist selection is adopted. The GA selects the individuals that optimize best the fitness function.
- c) The reproduction by crossover and mutation is then performed on the selected parents to generate two children that replace their parents in the new population. Mutation is carried out by randomly changing one or more genes (variables) of the created offspring. It is used for maintaining certain diversity in the population. The probability to perform the crossover and the mutation operator is specified as 0.75 and  $1/M$  respectively. The proposed algorithm applied the one-point crossover method as illustrated in Fig. 3

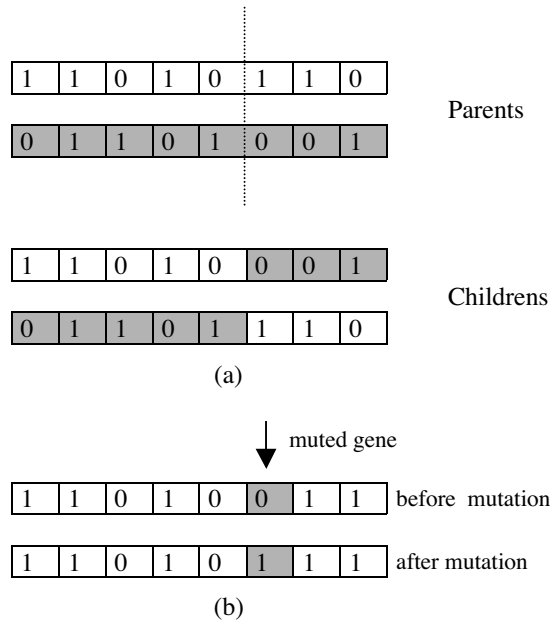


**Figure 3.** Operators of reproduction. (a) Crossover operator (b) Mutation operator.

According to the evolutionary theory, this new generation will be more adapted to the problem than the preceding one. The evolution optimization process is reiterated until satisfaction of a certain halting criterion or if a total number of generations is reached. A flowchart of the basic GA is shown in Fig. 4.

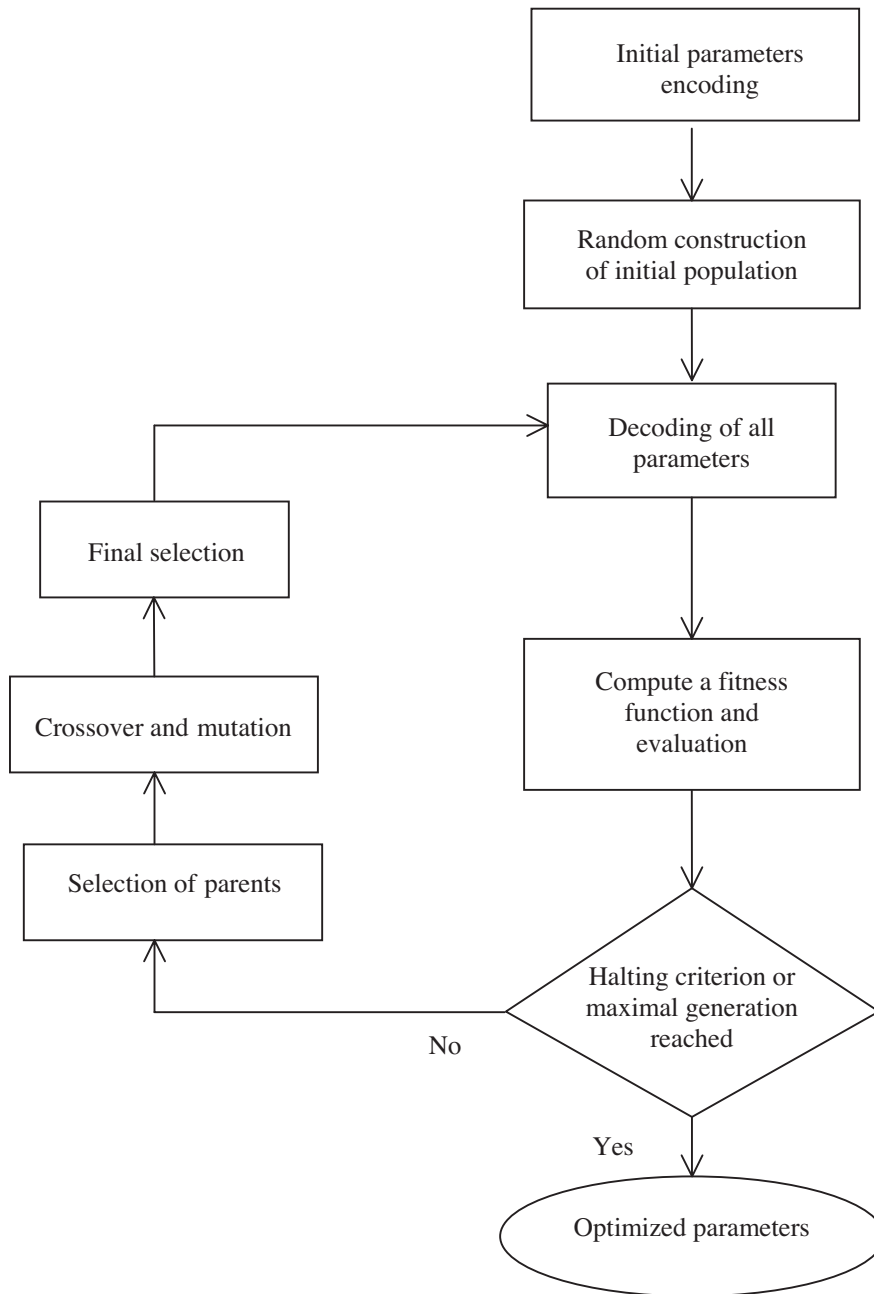


Figure 4. Flowchart for the GA.

Binary encoding is adopted. Each chromosome contains a number of genes, corresponding to a number of unknown variables. These variables are the geometrical parameters of the structure to optimize.

The coding of a variable  $x_k$  on an offspring of  $l_k$  bits implies a discretization of the research space in  $g_{k \max} = 2^{l_k} - 1$  discrete values,  $l_k$  is the length of the gene  $k$ . Geometrical parameters are decoded by the following equation [13]:

$$x_k = x_{k \min} + \left( \frac{x_{k \max} - x_{k \min}}{g_{k \max}} \right) \sum_{i=0}^{l_k-1} a_{ki} 2^i \quad (21)$$

where  $a_{k0}, a_{k1}, \dots$  are the  $l_k$  bits of the binary string representing  $x_k$ .  $x_{k \min}$  and  $x_{k \max}$  are the limits of the research interval, i.e.,

$$x_{k \min} \leq x_k \leq x_{k \max} \quad (22)$$

$x_{i \min}$  and  $x_{i \max}$  are determined by prior knowledge of the structure. It is necessary to fix these limits in order to avoid unreasonable parameters.

The resolution of a problem using GA requires representing the potential solutions of this problem in the form of chromosomes, to choose the suitable selective function and to define the genetic operators, which will be used. These operators, which are the population size, crossover rate and mutation rate, are important control parameters for GA. They affect the convergence to the optimal solution and computing time.

### 3. NUMERICAL RESULTS AND DISCUSSION

As a first application and in order to validate our analysis method, which is the mode-matching method, we present the study of inhomogeneous two and four-section transformers in circular waveguide. Fig. 6 and Fig. 8 (corresponding to the two and four-section transformer respectively) show the variation of the voltage standing waves ratio VSWR as a function of frequency (curves in dashed line; before optimization by GA) for the dominant  $TE_{11}$  mode in the useful band. The dimensions of the transformers are taken from reference [10]. Both transformers are quarter-wave, i.e., the length of sections are quarter-wave at design frequency  $f_0 = 9.5$  GHz. The convergence of the results is obtained using 10 modes in waveguides and 6 modes for the association of the  $S$  matrices. Our results are in good agreement with the reference [10]. Once the analysis algorithm is validated, we apply a genetic algorithm-based optimization process for optimizing the studied structures. The optimized transformers

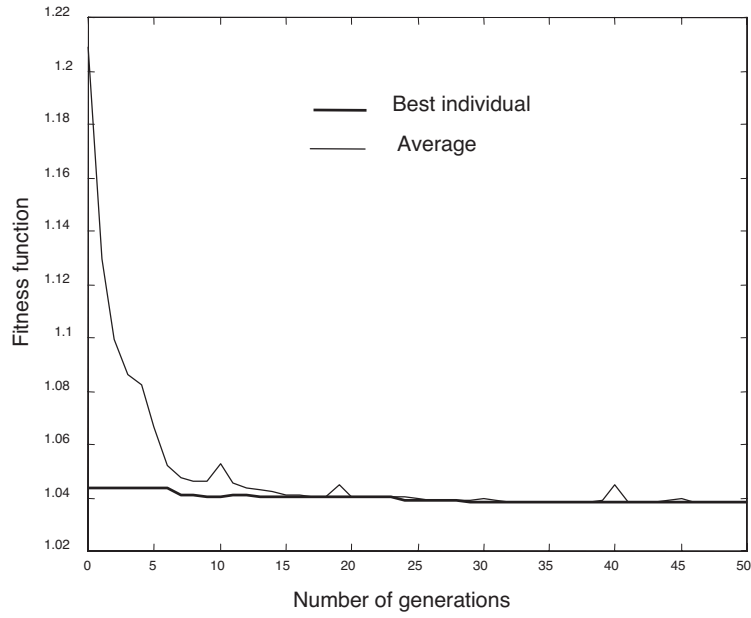


**Figure 5.** Evolution of fitness function for: the best individual and the average of fitness functions for structure 1.

**Table 1.** The dimensions in millimeters of optimized quarter-wave two and four-section transforms (structures 1 and 2).

	k	Ref.[10]	$R_k$ Obtained by GA	Ref.[10]	$l_k$ obtained by GA
Structure 1	0		11.165		$\infty$
	1	11.36	11.424	13.61	13.462
	2	11.965	12.172	12.41	12.152
	3		13.40		$\infty$
Structure 2	0		11.165		$\infty$
	1	11.21	11.226	13.99	13.943
	2	11.415	11.377	13.48	13.57
	3	11.685	11.856	12.93	12.628
	4	12.09	12.816	12.27	11.41
	5		13.40		$\infty$

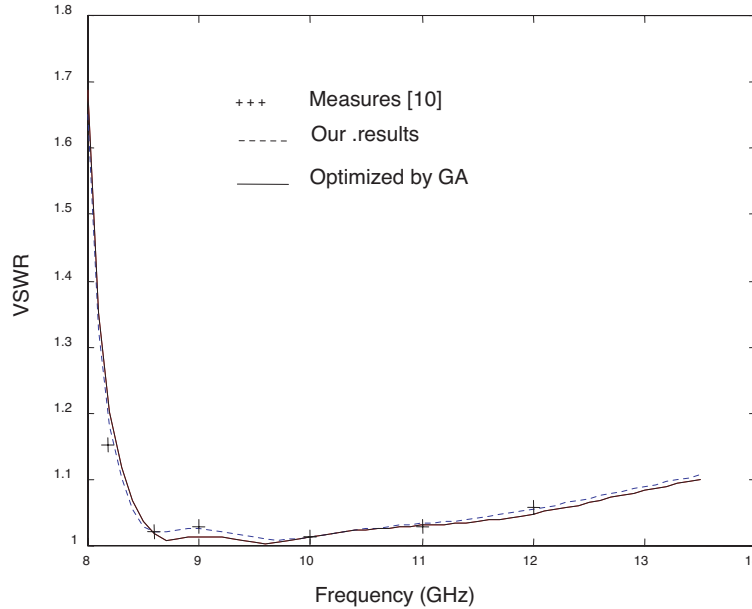


**Figure 6.** VSWR of optimized quarter-wave two-section transformer (structure 1). The corresponding dimensions are given in Table 1.

(curves in solid line) are compared to the inhomogeneous quarter-wave transformers modeled above. The input and output guides dimensions of the optimized transformers were fixed at reference values in order to always remain in the same frequency band, which is the useful band of the transformer. Constraints placed on the dimensions are fixed only by considerations for dominant mode propagation. It is assumed that the incident mode in the input guide is the dominant  $TE_{11}$  mode.

There are three points to take into account in the design of an optimum transformer: its length, its bandwidth and the tolerable reflection coefficient in the pass band [23].

Thus the purpose of optimization will be to minimize the voltage standing waves ratio (VSWR) near the design frequency, to decrease the overall length of the transformer and to increase its bandwidth. Since in the numerical resolution we have replaced the variation of the reflection coefficient by the variation of the voltage standing waves ratio, the fitness function became:

$$U' = \max_{f_{\min} < f < f_{\max}} [VSWR(f)]$$

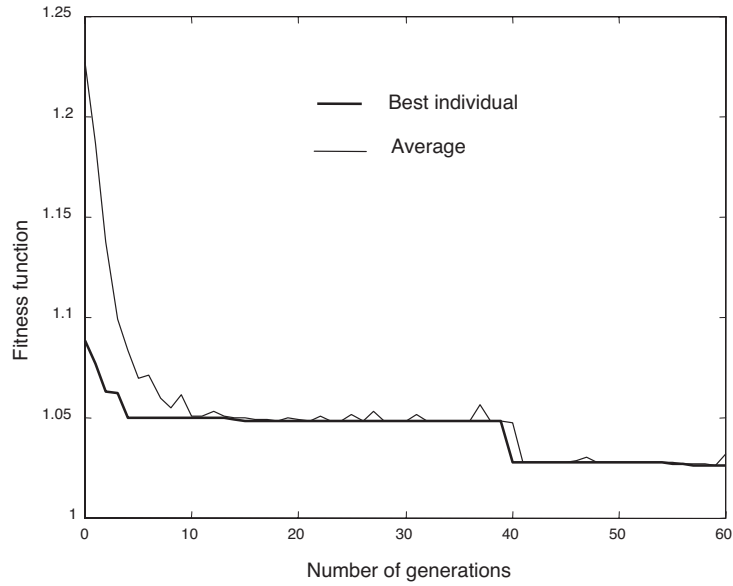


**Figure 7.** Evolution of fitness function for: the best individual and the average of fitness functions for structure 2.

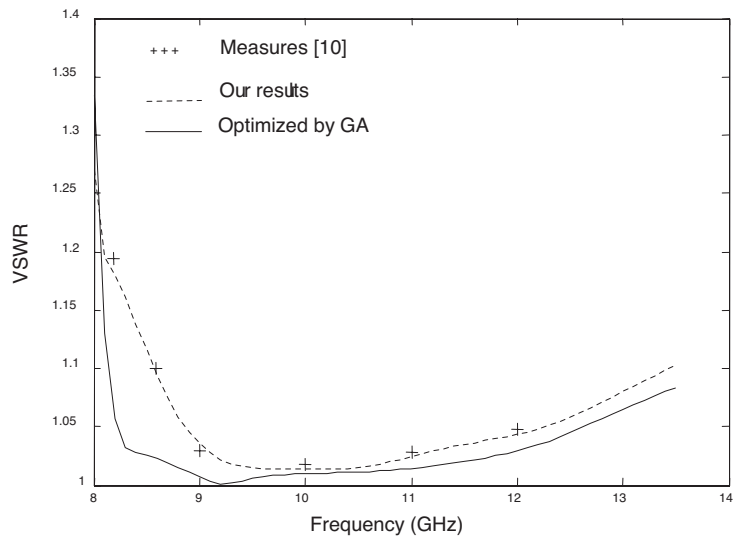


**Figure 8.** VSWR of optimized quarter-wave four-section transformer (structure 2). The corresponding dimensions are given in Table 1.

with

$$VSWR = \frac{1 + |S_{11}|}{1 - |S_{11}|}$$

for the dominant  $TE_{11}$  mode.

The genes constituting a chromosome correspond to the values of geometrical dimensions to optimize (radiuses and lengths of sections) of the studied structures.

The optimized transformers are quarter-wave at 9.5 GHz.

The geometrical parameters of a transformer with  $N$  sections must verify the following conditions:

$$\begin{cases} R_0 < R_1 < \dots < R_N < R_{N+1} \\ l_k = \lambda g_k / 4 \\ k = 1, 2, \dots, N \end{cases} \quad (23)$$

$R_0$  and  $R_{N+1}$  are respectively the radiuses of the input guide and the output guide, and  $\lambda g_k$  the guide wavelength of fundamental mode  $TE_{11}$  relating to the design frequency  $f_0 = 9.5$  GHz, and corresponding to the section  $k$ :

$$\lambda g_k = \lambda_0 / \sqrt{1 - (0.293\lambda_0/R_k)^2} \quad (24)$$

where  $\lambda_0 (= c/f_0)$  is the free space wavelength at 9.5 GHz. Only the dimensions  $R_k$  are optimized. The lengths  $l_k$  being fixed equal to the quarter of guide wavelengths of the corresponding sections. In practice, we treated two structures: the two-section transformer (structure 1) and the four-section transformer (structure 2).

The evolution of the fitness value for the more adapted individual and of the average of the fitness values as a function of the number of generations are represented in Fig. 5 and Fig. 7 respectively for structure 1 and structure 2. The population size was 30 individuals for structure 1 and 20 individuals for structure 2. Note that the individuals of the populations tend to identify with the better one. Fig. 6 and Fig. 8 represent the variation of the VSWR versus frequency for the dominant  $TE_{11}$  mode in the useful band of optimized quarter-wave transformers. The lengths of the sections are quarter-wave at 9.5 GHz.

The two-section transformer (Fig. 6) was optimized over the band 8.5 to 11.6 GHz. A maximum VSWR of 1.0384 was obtained. The VSWR is minimized near 9.5 GHz. A slight decrease in overall length was obtained.

For the four-section transformer (Fig. 8), all-round improvements in desired bandwidth, VSWR and overall length have been obtained. Table 1 shows the dimensions of the optimized transformers.



#### 4. CONCLUSIONS

This article presents the results of the design and optimization for two and four-section transformers in circular waveguides. An alternative method is used, which relies on a general fast electromagnetic analysis based on an optimization process. The design of a transformer with optimal frequential response requires the selection of the most relevant parameters with the aim of carrying out a maximum adaptation and satisfying certain design specifications. One possible approach for solving this problem is through the use of GA. It showed a great flexibility. A good choice of GA parameters, such as: the population size, the crossover rate and mutation rate accelerates convergence towards the optimal solution. Also, suitable choice of the search interval is a criterion of effectiveness in the search for the optimal solution.

Note that the use of GA adapts to the numerical responses provided by the mode-matching method and does not require a priori any assumption on the structure to be studied. This independence towards problems to be posed allows to the GA to be applied to an extremely wide range of problems.

#### REFERENCES

1. Guglielmi, M. and G. Gheri, "Rigorous multimode networks representation of capacitive steps," *IEEE Trans. Microwave Theory Tech.*, Vol. 42, 622–628, 1994.
2. Wilkins, G. M., J. F. Lee, and R. Mittra, "Numerical modeling of axisymmetric coaxial waveguide discontinuities," *IEEE Trans. Microwave Theory Tech.*, Vol. 39, 1323–1328, 1991.
3. Omar, A. S. and K. Schunemann, "Transmission matrix representation of finline discontinuities," *IEEE Trans. Microwave Theory Tech.*, Vol. MTT-33, 765–770, 1985.
4. Tao, J. W. and H. Baudrand, "Multimodal variational analysis of uniaxial waveguide discontinuities," *IEEE Trans. Microwave Theory Tech.*, Vol. 39, 506–516, 1991.
5. Scharstein, R. W. and A. T. Adams, "Thick circular iris in  $TE_{11}$  mode circular waveguide," *IEEE Trans. Microwave Theory Tech.* Vol. 36, 1529–1531, 1988.
6. Koshiba, M. and M. Suzuki, "Application of boundary-element method to waveguide discontinuities," *IEEE Trans. Microwave Theory Tech.*, Vol. MTT-34, 301–307, 1986.
7. Wexler, A., "Solution of waveguide discontinuities by modal

- analysis,” *IEEE Trans. Microwave Theory Tech.*, Vol. MTT-15, 508–517, 1967.
8. Sabatier, C., “Etude des discontinuités en guide circulaire à l’aide de l’analyse modale. Application aux cornets,” *Proc. JINA’88*, 432–436, 1988.
  9. Gesell, G. A. and I. R. Ciric, “Recurrence modal analysis for multiples waveguide discontinuities and its application to circular structures,” *IEEE Trans. Microwave Theory Tech.*, Vol. 41, 484–490, 1993.
  10. Sabatier, C., R. Behe, and P. Brachat, “Approximate formulas for step discontinuities in circular waveguides,” *Electron. Lett.*, Vol. 26, 173–175, 1990.
  11. Belmeguenai, M., M. L. Riabi, and P. Saguet, “Caractérisation rigoureuse des discontinuités en guides circulaires. Application aux iris et transformateurs,” *16th Int. Conference OHD’01*, 233–236, 2001.
  12. Goldberg, D. E., *Algorithmes Génétiques, Exploration, Optimisation et Apprentissage Automatique*, Addison-Wesley, France, 1994.
  13. Rahmet-Samii, Y. and E. Michielssen, *Electromagnetic Optimization by Genetic Algorithms*, Willey, New York, 1999.
  14. Allard, R. J., D. H. Werner, and P. L. Werner, “Radiation pattern synthesis for arrays of conformal antennas mounted on arbitrarily-shaped three-dimensional platforms using genetic algorithms,” *IEEE Trans. Antennas Propagat.*, Vol. 51, 1054–1062, 2003.
  15. Michielssen, E., J. M. Sajer, and R. Mittra, “Design of multilayered FSS and wave guide filter using genetic algorithms,” *IEEE AP-S Int. Symp. Dig.*, 1936–1939, 1993.
  16. Chiu, C. C. and W. T. Chen, “Electromagnetic imaging for an imperfectly conducting cylinder by the genetic algorithm,” *IEEE Trans. Microwave Theory Tech.*, Vol. 48, No. 11, 1901–1905, 2000.
  17. Lai, M. I and S. K Jeng, “Compact microstrip dual-band bandpass filters design using genetic-algorithm techniques,” *IEEE Trans. Microwave Theory Tech.*, Vol. 54, No. 1, 160–168, 2006.
  18. Nishino, T. and T. Itoh, “Evolutionary generation of microwaves lines segment circuits by genetic algorithms,” *IEEE Trans. Microwave Theory Tech.*, Vol. 50, 2048–2055, 2002.
  19. Bandler, J. W., “Computer optimisation of inhomogeneous waveguide transformers,” *IEEE Trans. Microwave Theory Tech.*, Vol. MTT-17, 563–571, 1969.
  20. Wade, J. D. and R. H. Macphie, “Scattering at circular-to-rectangular waveguide junctions,” *IEEE Trans. Microwave Theory*

- Tech.*, Vol. MTT-34, 1085–1091, 1986.
21. Chu, T. S. and T. Itoh, “Generalized scattering matrix method for analysis of cascaded and offset microstrip step discontinuity,” *IEEE Trans. Microwave Theory Tech.*, Vol. MTT-34, 280–284, 1986.
  22. De Smedt, R. and B. Denturk, “Scattering matrix of junction between rectangular waveguides,” *Proc. IEE H*, Vol. 130, 183–190, 1983.
  23. Riblet, H. J., “A general theorem on an optimum stepped impedance transformers,” *IRE Trans. Microwave Theorem Tech.*, 169–170, 1960.